Study of the residual stress field around Vickers indentations in a 3Y-TZP

Jérôme Chevalier, Christian Olagnon, Gilbert Fantozzi

Study of the residual stress field around Vickers indentations in a 3Y–TZP

J. CHEVALIER, C. OLAGNON, G. FANTOZZI
INSA GEMPPM, URA 341, 69621 Villeurbanne Cedex, France

Indentation cracks are often used as initial flaws in ceramics for different mechanical tests because of their unique advantages. The residual stresses around the indent due to the elastic/plastic contact must generally be relaxed, which can be conducted by heat treatment. The stress field around Vickers indentation and conditions of annealing have been analysed on a Y–TZP material. Different heat treatments from room temperature up to 1200 °C have been conducted. The residual stress field has been characterized by different methods. First, stable crack propagation in the residual stress field has been conducted by applying a bending stress to the indented specimens. The apparent toughness has also been measured by conducting fast fracture on indented specimens. Finally the residual stress present around the indentation has been measured by making micro-indentations and by measuring the crack lengths. The results show that at intermediate temperatures up to 600 °C an apparent stress relaxation occurs due to the tetragonal to monoclinic phase transformation which induced a superimposed compressive stress. The higher temperature of 1200 °C effectively leads to a real stress relaxation without healing the crack.

1. Introduction

Indentation flaws are widely used for the mechanical behaviour characterization of dense ceramics. They present several advantages: (i) a very well defined geometry, (ii) a precise knowledge of crack parameters due to numerous fracture mechanics analyses [1–3], and (iii) a high reproducibility of size and shape. Indentation flaws, and especially Vickers flaws are therefore conveniently used to induce critical flaws in small 4-point bending specimens to characterize the toughness or the sub-critical crack growth behaviour of ceramic materials.

The description of the material around a Vickers indentation was shown to be complex. It is generally considered as a hemispherical plastic zone beneath the indenter, surrounded by the elastic body. The elastic/plastic contact generates residual stresses around the indentation, acting as an additional crack driving force during bending (or any other applied stress) tests.

Theoretical models and experimental investigations have allowed the understanding of the impact of the residual stress on this additional driving force. It is now well established [3] that the residual stresses lead to a residual stress intensity factor on each crack in the form of:

$$K_{res} = \chi P a^{-3/2} \quad (1)$$

where a is the crack size induced by the indentation, P is the load applied to the indenter and χ is a constant of the material which depends on the Young's modulus to hardness ratio. The value of χ has been the subject of many hypotheses to evaluate the toughness.

Recently, Pajares and co-workers [4, 5] and Kurth *et al.* [6] have developed a novel method to determine the toughness using the stable propagation of indentation cracks. An important advantage of this method is to directly measure the χ parameter without restrictive assumption. This allows one to take into account the residual crack driving force and to obtain accurate values of the toughness.

For sub-critical crack growth measurements (static fatigue, dynamic fatigue and cyclic fatigue), in which indentation flaws are introduced, the analysis generally does not take into account this residual stress intensity factor. It is however clear that owing to this residual stress around the indent no accurate lifetimes and consequently no relevant propagation law can be obtained [7].

An established method to reduce this residual stress intensity factor is to recover it by a thermal treatment. In the case of ceramics that do not exhibit a phase transformation (e.g. Al_2O_3, Si_3N_4, SiC, mullite, etc.) the recovery is due to both dislocation movement and/or grain boundary sliding that can be assisted by diffusion. Therefore, long duration and high temperature annealings are required to suppress or reduce this residual stress. The case of zirconia-based ceramics is different since transformation plasticity occurs and acts as an additional plastic deformation contribution. Transmission electron microscopy (TEM) characterization of an indented polycrystalline Y–PSZ [8] has shown that the microstructure around the indentation consists of a transformed zone and another region having a high dislocation density. Experiments on a yttrium-stabilized zirconia single

crystal [9] have shown that many slip systems are activated, but it has also been shown in a polycrystalline 3Y–TZP that a large transformed zone was present after indentation.

Pajares *et al.* [5] have clearly demonstrated that short times and relatively low temperatures ($< 400\,^{\circ}C$) can reduce the residual stress intensity factor. It has however not been proved that the residual stress was actually annealed for these short time ageings and no correlation with microstructure has been made. On the other hand, Wang and Stevens [10] have demonstrated that a 1250 °C for 20 min heat treatment altered the indentation prints. They considered that it was not only due to annealing of the residual stress but that crack healing could occur by diffusion mass transport.

The aim of this paper is to better understand the effect of annealing on the residual stress intensity factor and on the microstructure modification and to correlate them. The aim is also to determine a heat treatment that could reduce the residual stress intensity factor without healing the crack.

For this purpose, different methods have been used to characterize the stress field around indentation cracks in 3Y–TZP materials. The method proposed by Pajares *et al.* [4] was used to determine K_{Ic} and χ after heat treatments between 20 to 1200 °C. The measurement of the apparent toughness in a fast fracture bending test was conducted after the same treatments. The residual stress has been directly measured by a micro-indentation method [11].

2. Experimental procedure

2.1. Material

The material studied in this work was a 3Y–TZP sintered at 1450 °C. A density of $6.06\,g\,cm^{-3}$ was measured by Archimedes method and the average grain size was 0.58 μm. Bending bars of dimensions $3\,mm \times 4\,mm \times 40\,mm$ were ground and polished down to 1 μm grit. The specimens were subsequently heat treated at 1200 °C for 1/2 h. Indentations were subsequently made on one face of the specimens. The post-indentation treatments were conducted at various temperatures from 20 up to 1200 °C for 12 min.

2.2. Controlled propagation of indentation cracks [5, 6]

Indentation flaws were made on polished 4-point bending bars by a Vickers indenter by applying a load of 100 N. Indentation cracks were shown to be approximately halfpenny-shaped and the length measured by an optical microscope was found to be of 144 ± 2 μm.

When loading these bars in bending the cracks are submitted to a two-fold stress field: (i) the applied stress σ_{app}, and (ii) the residual stress σ_r. They are therefore submitted to the total driving stress intensity factor K_{Itot} of the form:

$$K_{Itot} = K_r + K_{app} = \chi P a^{-3/2} + Y\sigma_{app} a^{1/2} \quad (2)$$

where Y is a parameter that depends on the type of crack and loading. Its value for a halfpenny crack has been evaluated by Smith *et al.* [12]. The crack propagation occurs if the total stress intensity factor K_{Itot} matches the material toughness K_{Ic}, but a stable propagation is expected as long as the condition:

$$\frac{dK_{Itot}}{da} < 0 \quad (3)$$

is fulfilled. Under these conditions and the assumption of a constant Y parameter, Equation 2 can be rearranged to a linear form as:

$$Y\sigma_{app} a^{1/2} = K_{app} = K_{Ic} - \chi P a^{-3/2} \quad (4)$$

Therefore by plotting the applied stress intensity factor versus $\chi P a^{-3/2}$ one can obtain the two parameters χ and K_{Ic}. This can be achieved by recording the applied stress and the crack length during a stable propagation experiment.

For this purpose, indented specimens were loaded at high loading rate ($8000\,N\,s^{-1}$) to prevent sub-critical crack growth, and subsequently unloaded at the same rate. The crack length was further measured by optical microscopy with a precision of ± 2 μm. The same procedure was repeated several times by increasing the load until specimen failure due to crack instability. This measurement has been achieved both on as-indented specimens and after annealing.

2.3. Apparent toughness measurement

The toughness is generally measured by recording the fracture stress on a specimen containing a defect of known size and shape, by applying the standard formula:

$$K_{Ic} = Y\sigma a^{1/2} \quad (5)$$

This can be done in bending on an indented specimen after measuring the crack length. However, since the above equation does not take into account the influence of the residual stress, only an apparent toughness lower than the real value will be measured. The apparent toughness has been measured on a series of indented specimens tested in 4-point bending after various annealing treatments (as defined in Section 2.1). The displacement rate was $5\,mm\,min^{-1}$, and the apparent critical stress intensity factor evaluated by Equation 5 with $Y = 1.34$ [12] and by considering the initial crack length before the test, the sub-critical crack growth being considered as negligible. Three specimens were used for each heat treatment. The measured apparent toughness was compared to the real value obtained from Section 2.2.

2.4. Stress measurement by micro-indentation method

Indentation flaws can be used to analyse residual stress fields in materials. The basis of the method is that indentation induced cracks are submitted to a two-fold stress field: the stress due to the indentation itself and the residual stress σ_{res}. Recalling that the

stable crack propagation stops at $K_{Itot} = K_{Ic}$ (for $dK_{Itot}/da < 0$), the probe indentation crack length will be given by the equation:

$$K_{Ic} = Y\sigma_{res}\, a^{1/2} + \chi P' a^{-3/2} \quad (6)$$

where P' represents the probe indentation load. The residual stress to analyse can therefore be expressed as:

$$\sigma_{res} = \frac{K_{Ic} - \chi P' a^{-3/2}}{Y a^{1/2}} \quad (7)$$

The toughness can be expressed as a function of the crack length obtained in a stress free material, a_0, as $K_{Ic} = \chi P a_0^{-3/2}$ which can be substituted in Equation 7 leading to:

$$\sigma_{res} = K_{Ic} \frac{1 - (a/a_0)^{-3/2}}{Y a^{1/2}} \quad (8)$$

This method proposed by Chantikul *et al.* [13] has recently been used to characterize the stress field around an indentation (macro) in glass [14] by using small indentations (micro) as a probe.

In this work a similar procedure has been achieved to investigate the evolution of the residual stress as a function of the heat treatment.

Macro-indentations were made on a polished specimen at a load of 625 N and several annealing treatments were conducted. Micro-indentation probes were subsequently made at a load of 50 N around the macro-indentation and the residual stress, considered as constant has been evaluated from Equation 8.

Previous analyses [3] of the residual stresses around an indentation have shown a central symmetry at the surface characterized by the two principal stresses, radial (σ_R) and tangential (σ_T). By carefully aligning the probe indentations along the radial direction (cf. Fig. 1) the two components could be directly obtained from the different crack lengths. This procedure requires the knowledge of the toughness which was selected as $K_{Ic} = 7.2\ \text{MPa m}^{1/2}$ (value presented in the Sections 2.2 and 2.3).

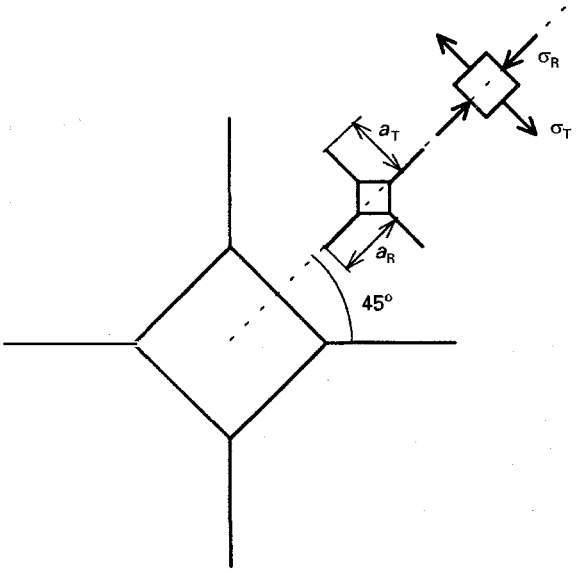

Figure 1 Schematic drawing showing the procedure conducted to evaluate the stress field around a macro-indentation, by the micro-indentation technique.

3. Results and discussion

3.1. Stable propagation of indentation cracks

Fig. 2 shows the plot of $(Y\sigma a^{1/2})$ as a function of $(Pa^{-3/2})$ for different bending bars. Different behaviours are observed.

In the case of as-indented specimens, the curve is linear indicating that the stress field due to indentation follows the expected form given by Equation 1. It can also be considered that Y is constant over the crack length investigated. This graph also shows that the onset of crack propagation begins for a threshold stress intensity factor $K_{app} = 1.9\ \text{MPa m}^{1/2}$, for an initial measured crack length of $a_{im} = 144\ \mu\text{m}$. This offset value which indicates that the starting total stress intensity factor (K_{Itot}) is lower than the toughness (K_{Ic}) will be explained further in the paper. The fitting of the curve by a straight line gives: $K_{Ic} = 7.25\ \text{MPa m}^{1/2}$ and $\chi = 0.0925$.

In the case of the specimens annealed up to 200 °C, a stable crack propagation could be obtained. This indicated that the residual stress was still present in the specimen. The data define a straight line which shows that the residual component can again be described by Equation 1, but with a lower slope when expressed by Equation 4. It is also important to note that the stress intensity factor offset is more prominent with a value of $K_{offset} = 4\ \text{MPa m}^{1/2}$. The fitting of the data by a straight line leads to $K_{Ic} = 7.25\ \text{MPa m}^{1/2}$ and $\chi = 0.0626$. There is therefore an apparent stress relaxation suggested by the reduction of χ and the increase of K_{offset}.

An annealing treatment at room temperature for 7 days plays a similar role as a 200 °C heat treatment. This suggests an apparent stress relaxation around the indentation at ambient temperature.

The behaviour of the specimens annealed at a temperature in the range 400 to 800 °C is different. No stable propagation could be obtained, but it can be noted that failure is obtained at a stress intensity factor lower than the fracture toughness. The recorded

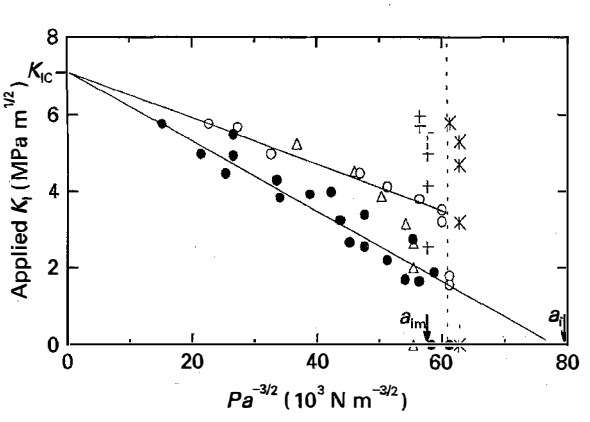

Figure 2 Plot of the applied stress intensity factor as a function of $Pa^{-3/2}$ during a controlled propagation of an indentation flaw on a bending bar after several treatments: (●) as-indented; (○) annealed at 200 °C, (+) annealed at 400 °C; (*) annealed at 600 °C (△) annealed at room temperature for 1 week.

offset values of the stress intensity factor were 6.0 MPa $m^{1/2}$ at 400 and 800 °C.

Theoretical analyses show that the initial crack length a_i obtained just after indentation is given by:

$$K_{Ic} = \chi P a_i^{-3/2} \quad (9)$$

The extrapolation of the graph $Y\sigma a^{1/2} = f(Pa^{-3/2})$ for null stress values theoretically leads to the value of a_i given by Equation 9 which is here equal to 116 μm, i.e. lower than the experimental measurement. Anstis *et al.* [2] have pointed out that Equation 9 is not valid if sub-critical crack growth occurs after indentation. In previous studies [14, 15], it has been shown that Y–TZP was sensitive to sub-critical crack growth in air. Thus the presence of the K_{offset} at room temperature could be explained by the sub-critical crack growth which would lead to a longer initial crack submitted to a stress intensity factor due to residual stress lower than K_{Ic}. The condition of controlled crack propagation would therefore not be obtained at the onset of loading. It could also be argued that a partial stress relaxation occurs at room temperature, which also would lead to an offset.

The first assumption has been verified by indenting a specimen in silicon oil which effectively prevents extensive sub-critical crack growth. The measurement of this crack after indentation gave a value of 114 μm. This proves that the cause of the offset at room temperature is the immediate crack propagation subsequent to indentation.

For samples heat treated between 400 and 800 °C, no stable propagation occurs, even with careful loading. However, the residual stress is not fully relaxed since the offset stress intensity factor was below the toughness. This apparent contradiction already mentioned by Pajares *et al.* [5] can be explained as follows:

It is first assumed that the residual stress intensity factor is still of the form given by Equation 1. For each heat treatment temperature, χ can be determined either by linear regression for room temperature and 200 °C or from the measurement of the K_{offset} for temperatures of 400 and 800 °C. In this last case, the χ value is obtained from the offset value (corresponding to unstable crack propagation) and from Equation 4. The values are reported in Table 1.

The crack stability analysis in this type of test shows that an instability point (i.e. $dK_{Itot}/da \geqslant 0$ and $K_{Itot} = K_{Ic}$) is obtained for a critical value of crack length a_c given by [2]:

$$a_c = (4\chi P/K_{Ic})^{2/3} \quad (10)$$

By replacing the different values of χ corresponding to the different temperature treatments one can evaluate the critical crack length leading to unstable crack propagation (Table I). It appears that for the temperatures of 400 and 800 °C these critical values are smaller than the initial measured value a_{im}. This explains why no stable propagation could be obtained although a residual stress is still present. This shows that the presence of a residual stress is not a sufficient condition for having a stable crack propagation in this test, but that the initial crack length obtained after indentation must be smaller than the critical crack length a_c.

TABLE I Values of the residual stress constant and the critical crack length for both stable and unstable crack propagation

	χ	a_c (μm)
Ambient	0.0925	296
200 °C	0.0626	229
400 °C	0.023	117
800 °C	0.023	117

3.2. Apparent toughness measurements

Fig. 3 represents the measured apparent toughness as a function of the heat treatment temperature. The shape of the curve is rather complicated and two plateaus are observed, respectively, between 400 and 800 °C, and between 1000 and 1200 °C. It immediately appears that for temperatures lower than 1000 °C the apparent toughness is lower than the toughness indicating that the residual stress has not been relaxed. On the other hand, heat treatments up to 1400 °C lead to an apparent toughness higher than the real toughness. As already mentioned by Wang and Stevens [10], this phenomenon can be due to crack healing by diffusion because the temperature is close to the sintering temperature. This can be confirmed by microscopic observations which show a crack length decrease.

Heat treatments between 1000 and 1200 °C seem however relevant for effective stress relaxation. The understanding of the behaviour has been achieved by optical microscopy in Normarsky interferences which reveals the surface displacement due to indentation (Fig. 4). It should be noted that heat treatments result in a surface displacement around the indents. Behrens *et al.* [16] have shown that this displacement is a consequence of a stress assisted tetragonal to monoclinic (t → m) transformation around the indent which results in a volume increase.

Up to 400 °C, an increase in the monoclinic content around the indentation is observed.

The first two parts up to 800 °C of the curve in Fig. 3 can therefore be explained by this t → m transformation. Indeed, it might be supposed that the

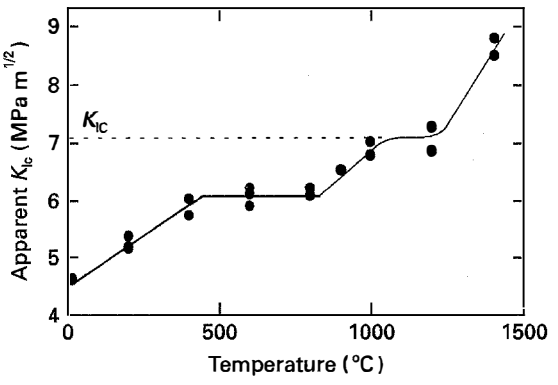

Figure 3 Apparent toughness as a function of the annealing temperature, measured in bending using the crack size measured just after indentation.

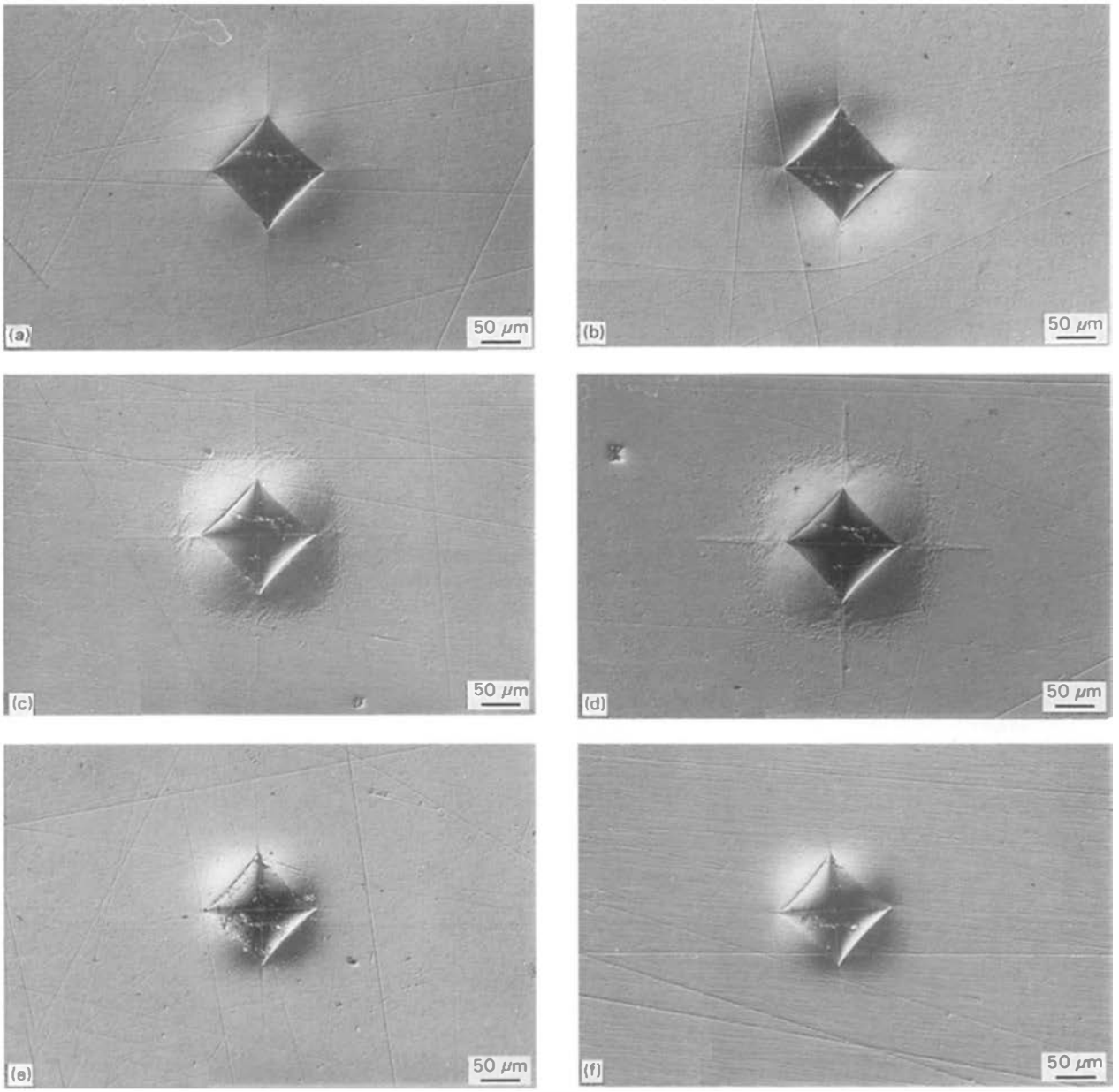

Figure 4 Optical micrograph in Normasky interference contrast of Vickers indentations after different heat treatment temperatures: (a) no treatment, just after indentation, (b) 200 °C, (c) 400 °C, (d) 800 °C, (e) 1000 °C, and (f) 1200 °C. Bar scale represents 50 μm.

t → m transformation leads to a compressive stress that hinders the initial residual stress. It can also be assumed that this transformation does not lead to a real stress relaxation, but only acts as a superimposed compressive stress. This will be addressed in the following section.

The shape of the curve between 800 and 1200 °C can not be explained by the transformation induced stress at the surface since the monoclinic content decreases. The possible mechanisms will be discussed in the following section. Note however that a real stress relaxation occurs in this temperature range because the apparent toughness matches the real toughness value and the surface monoclinic content is negligible.

3.3. Residual stress measurements

Fig. 5 shows the stress profiles around indentations. It appears that the radial stresses are compressive while the tangential stresses are tensile components, in agreement with theoretical analyses. It should be noted that the compressive component is higher but does not contribute to the crack advance. The main limit of this method is the impossibility to measure stresses in the region very near to the indentation. Indeed, in this case, the tangential secondary cracks are closed and one of the radial secondary cracks is connected to the macro-indentation, which prevents any measurement (cf. Fig. 6a).

The stress profiles for specimens annealed between 200 and 800 °C are also represented in Fig. 5. The radial component of the stress is unchanged in the explored range. Note also that measurements of a_T were not possible in the high monoclinic content region. Tangential stresses have been modified in this range of heat treatments. It is important to recall that this corresponds to heat treatments that induced a strong t → m transformation that led to an

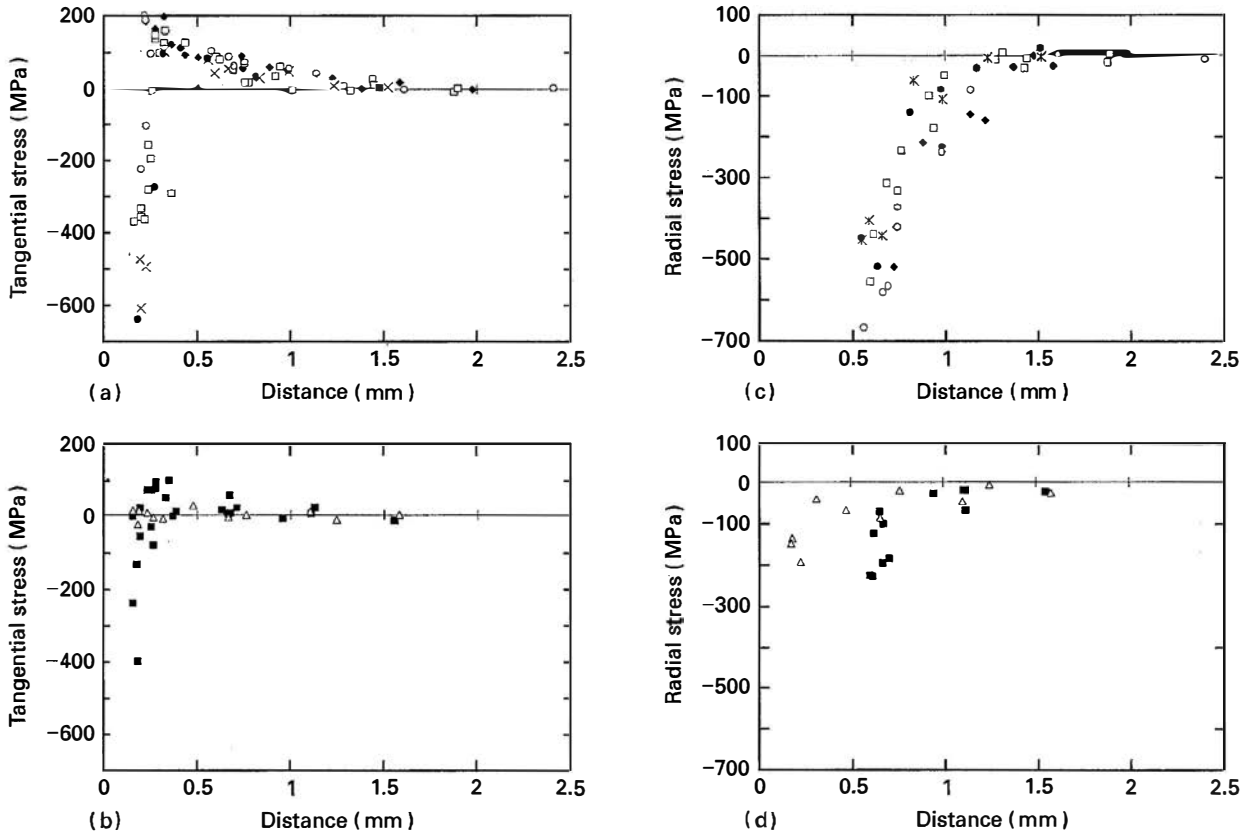

Figure 5 Surface tangential (a) and (b), and radial (c) and (d) stresses as a function of the distance from the centre of an indentation after different annealing treatments. Key: ◆ as-indented; ○ 200 °C; □ 400 °C; ×, ∗ 600 °C; ●800 °C; ■ 1000°C; △ 1200 °C.

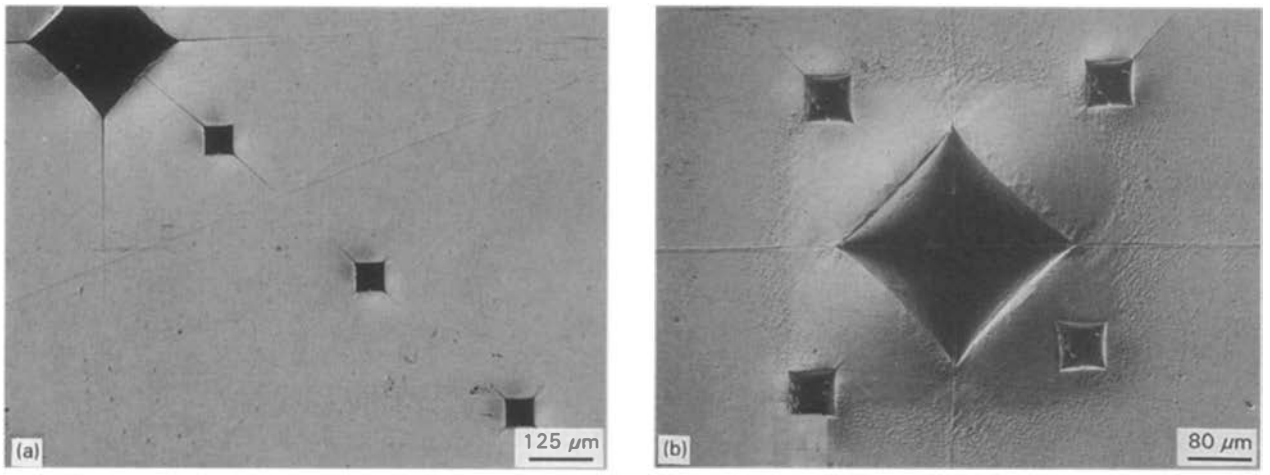

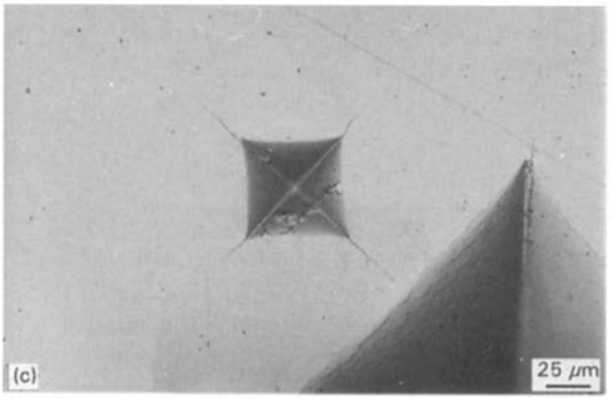

Figure 6 Optical micrograph showing the probe indentation around the main indentation. (a) Main indentation with different micro-indentation probes, (b) after 600 °C annealing treatment, showing the superimposed compressive stress, and (c) after 1200 °C heat treatment, showing the absence of residual stress.

additional compressive stress. The tangential stress is therefore the sum of two components, a tensile stress resulting from the indentation and a compressive stress resulting from the temperature induced phase transformation. This can be confirmed by noting that the compressive stress is only present in a limited area around the centre of the indent. Outside this area the tangential component is the same as it was before the heat treatment. This can also be illustrated by Fig. 6b where it is observed that an indentation made in the

compressive region induced no crack neither in the radial nor in the tangential direction.

The increase of apparent K_{Ic} with temperature in the range of 200 to 600 °C in the previous experiments is therefore clearly due to the increase of this additional compressive stress and it is definitely not a relaxation phenomenon.

The stress measurement profiles of specimens heat treated at temperatures over 800 °C are also represented in Fig. 5. It is observed that the compressive radial stress due to the t → m transformation has disappeared. In this temperature range, the tetragonal phase is stable. Both the radial and the tangential components of the residual stress have been reduced. The tangential component is even fully relaxed between 1000 and 1200 °C. This therefore explains why the apparent toughness is equal to the real toughness since there is no residual stress. This is illustrated in Fig. 6c.

The mechanism responsible for this real relaxation can be either due to dislocation movement or to m → t transformation. Indeed, Pajares *et al.* [8] have observed on an indented Y–TZP that the microstructure associated with indentation consists of a large hemispherical transformed monoclinic zone under the indentation print, and a region containing a high density of dislocations. Behrens *et al.* [16] have shown on a 3Y–TZP that a significant t → m transformation occurs below the indenter after indentation. Stress relaxation can therefore be due to the reversible m → t in the range 1000 to 1200 °C, or to the dislocation movement as in other non-transforming ceramics. It can be noted that at 1200 °C and for the relatively limited treatment ageing times (12 min) conducted in this work, dislocation movements are probably limited [9] and the relaxation is probably due to the m → t transformation below the indent. Furthermore the diminution of the amount of monoclinic phase at the surface corresponds to the phase diagram transformation.

4. Conclusion

An analysis of indented Y–TZP specimens that have been heat treated for 12 min over a wide range of temperatures has been carried out. Three different tests have been conducted: apparent toughness measurement fast fracture, stable crack propagation and measurement of the residual stress by indentation method.

Experiments conducted on as-indented samples have shown that the residual stress intensity factor K_r could be expressed by the relation $K_r = \chi P a^{-3/2}$, in which the constant χ has been determined.

Heat treatments up to 800 °C lead to an apparent stress relaxation which actually is due to the appearance of a t → m transformation induced compressive stress near the indentation. The resulting stress field leads to a decrease of the residual stress intensity factor and therefore to an increase of the apparent toughness.

Between 800 and 1200 °C, the reversible m → t transformation and possibly dislocation movements lead to real stress relaxation.

Above 1200 °C, crack healing due to diffusion occurs and modifies the crack pattern.

Finally an annealing treatment at 1200 °C for 12 min leads to a total stress relaxation around the indent without crack healing. Such a treatment is therefore relevant to prepare indented specimens in Y–TZP materials without residual stress for any subsequent mechanical tests such as static or cyclic fatigue.

Acknowledgement

The authors wish to thank Dr. Bernard Calès and Ceramiques Techniques Desmarquest (France) for supplying the material and for their financial support.

References

1. R. COOK and G. PHARR, *J. Amer. Ceram. Soc.* **73** (1990) 787.
2. G. R. ANSTIS, P. CHANTIKUL, B. R. LAWN and D. B. MARSHALL, *ibid.* **64** (1981) 533.
3. B. R. LAWN, "Fracture of Brittle Solids", 2nd Edn, Cambridge Solid State Science Series (Cambridge University Press, Cambridge, 1993).
4. A. PAJARES, F. GUIBERTEAU, A. DOMINGUEZ-RODRIGUEZ, G. DRANSMANN, R. W. STEINBRECH, in Proceedings of the Second Euro Ceramics, Vol. 2, Aylesburg 1991, edited by G. Ziegler and H. Hausner, pp. 1023–1030.
5. A. PAJARES, F. GUIBERTEAU, A. DOMINGUEZ-RODRIGUEZ, G. DRANSMANN, Y. STOCKMAN and R. W. STEINBRECH, in Proceedings of the Third Euro Ceramics, Vol. 3, 1993, edited by P. Durand and J. F. Fernandez, pp. 531–36.
6. R. KURTH, G. KLEIST and R. W. STEINBRECHT, in Proceedings of the Third Euro Ceramics, Vol. 3, 1993, edited by P. Durand and J. F. Fernandez, pp. 853–58.
7. S. Y. LIU and I. W. CHEN, *J. Amer. Ceram. Soc.* **74** (1991) 1206.
8. A. PAJARES, F. GUIBERTEAU, K. H. WESTMACOTT and A. DOMINGUEZ-RODRIGUEZ, *J. Mater. Sci.* **28** (1993) 6709.
9. G. MORSCHER, P. PIROUZ and A. HEUER, *J. Amer. Ceram. Soc.* **174** (1991) 491.
10. J. WANG and R. STEVENS, *J. Mater. Sci. Lett.* **7** (1988) 560.
11. K. ZENG and D. ROWCLIFFE, *J. Amer. Ceram. Soc.* **77** (1994) 524.
12. F. W. SMITH, A. F. EMERY and A. S. KOBAYASHI, *J. Appl. Mech. ASME*, December (1967) N° 67-WA/APM-2.
13. P. CHANTIKUL, D. B. MARSHALL, B. R. LAWN and M. G. DREXAGE, *J. Amer. Cerami Soc.* **62** (1979) 551.
14. J. CHEVALIER, C. OLAGNON and G. FANTOZZI, in Proceedings of the 3rd European Ceramic Society Conference, Madrid(SP), September 1993, Vol. 3, pp. 871–76.
15. M. KNECHTEL, D. GARCIA, J. RÖDEL and N. CLAUSSEN, *ibid.* **76** (1993) 2681.
16. G. BEHRENS, G. W. DRANSMANN and A. HEUER, *ibid.* **76** (1993) 1025.